Assessing the structural integrity of the wax-resin lining of The Night Watch using 3D shearography

Tao, Nan; van Duijn, Esther; Vos, Lisette; Steeman, Ilse; Groves, Roger M.; Keune, Katrien; Noble, Petria; Anisimov, Andrei G.

DOI
10.1016/j.culher.2025.02.002

Publication date
2025

Document Version
Final published version

Published in
Journal of Cultural Heritage

Journal of Cultural Heritage 72 (2025) 169–179

Contents lists available at ScienceDirect

Journal of Cultural Heritage

journal homepage: www.elsevier.com/locate/culher

Original article

Assessing the structural integrity of the wax-resin lining of *The Night Watch* using 3D shearography

Nan Tao[a,*], Esther van Duijn[b], Lisette Vos[b], Ilse Steeman[b], Roger M. Groves[a], Katrien Keune[b,c], Petria Noble[b], Andrei G. Anisimov[a]

[a] *Department of Aerospace Structures and Materials, Delft University of Technology, Delft 2629 HS, The Netherlands*
[b] *Conservation & Science Department, Rijksmuseum, Museumstraat 1, 1070 DN, Amsterdam, the Netherlands*
[c] *Van't Hoff Institute for Molecular Sciences, University of Amsterdam, Amsterdam 1090 GD, The Netherlands*

ARTICLE INFO

Article history:
Received 4 October 2024
Accepted 3 February 2025
Available online 15 February 2025

Keywords:
Wax-resin relining
Structural treatment of canvas paintings
3D shearography
Delamination
Non-destructive inspection
The Night Watch

ABSTRACT

Assessing the structural integrity of cultural heritage objects is of great importance for their structural conservation and long-term preservation. This paper focuses on the development of a non-destructive inspection (NDI) approach using 3D shearography to evaluate the structural integrity of wax-resin lined paintings, specifically for *The Night Watch* (1642), a large-format 17th-century canvas painting by Rembrandt van Rijn (1606–1669) that is on display in the Rijksmuseum, Amsterdam. *The Night Watch* has a complex treatment history that has many old repairs of structural defects and damages (holes, tears, etc.) and three wax-resin relinings. In 2021, before a new structural intervention involving retensioning of the canvas support, it was vital to evaluate the structural integrity of the painting, specifically the condition of the treatment carried out in 1975–76 when, among other actions, several long cuts in the area of Captain Frans Banninck Cocq's breeches were repaired and an old canvas insert in the drum was replaced. To assess the structural condition, we applied 3D shearography to quantitatively analyse the in- and out-of-plane surface strains with controlled thermal loading. First, a safe loading procedure was developed by inspecting a representative wax-resin lined test painting where reference delaminations and structural repairs to canvas supports were reliably identified with 3D shearography by raising the temperature with 1-2 °C. As part of Operation Night Watch, in November 2021 an in-situ investigation was carried out in the Rijksmuseum gallery. Two areas of interest in *The Night Watch*, the restored slashes in the Captain's breeches (0.5 × 1 m) and the canvas insert in the drum (0.2 × 0.5 m), were inspected from the reverse of the painting. Results revealed no critical structural problems associated with the repaired slashes, nor with adhesion of the lining. For the patched canvas in the drum, it showed higher in- and out-of-plane strain variations. Overall, 3D shearography provided valuable non-destructive inspection results for assurances regarding the structural integrity of the 1975 repairs and the adhesion of the lining canvas in *The Night Watch*.

1. Research aim

The aim of this study is to assess the structural integrity of the wax-resin lining of Rembrandt's *The Night Watch* (1642), using 3D shearography with thermal loading. This work started with inspection of a lined test painting with controlled damage in the laboratory environment and progressed to an in-situ investigation of *The Night Watch* in the Rijksmuseum gallery. The previously developed 3D shape shearography system was adapted, enabling the full field monitoring of large-scale wax-resin relined paintings in both in- and out-of-plane strain fields. A safe loading procedure for paintings during the inspection, including exposure to light and the increase of the canvas temperature, was also developed.

2. Introduction

Assessing the structural integrity of cultural heritage objects is important for the success of conservation interventions and an artwork's long-term preservation. Canvas paintings, which invariably have incurred various interventions and damages from their centuries of existence, usually have complex treatment histories [1]. This can include the repair of tears and holes, tacking edges and relinings, all of which potentially can affect the ability of a painting

* Corresponding author.
E-mail address: n.tao@tudelft.nl (N. Tao).

https://doi.org/10.1016/j.culher.2025.02.002

to hold together under a load, including its own weight, without deforming. In particular, wax-resin relinings, which correspond to the impregnation of the entire structure with molten wax and resin and bonding of an additional canvas to the back of the original canvas, have commonly been used to strengthen paintings in the past [2,3]. Various defects and damage (e.g., cuts and delaminations) may occur in paintings due to vandalism acts, fluctuations in temperature and humidity, and artwork transportation [4,5]. The risk of occurrence depends on the object's materiality, how it was made, and its conservation history. The focus of this study is *The Night Watch* (1642), a large-format canvas painting by Rembrandt van Rijn that is on display in the Rijksmuseum, Amsterdam. *The Night Watch* has a complex treatment history including several cleanings and restorations, varnish treatments and relinings [1,6–8]. In 1975, the canvas was slashed twelve times by a visitor with a serrated dinner knife, including several slashes of almost a meter long in the area of Captain Frans Banninck Cocq's breeches. During the subsequent structural treatment in 1975–76 and restoration of the painting, the long slashes were repaired and the painting was relined with an additional canvas using a mixture of beeswax and resin. An old canvas insert in the drum of about 6×9.5 cm was also replaced [7,8]. Consequently, in 2021 prior to a proposed new structural treatment involving retensioning of the canvas support [9], it was important to evaluate the structural integrity of these regions of the painting, which is the main aim of this study. However, to date, there is no standard instrument or procedure to evaluate the structural integrity of wax-resin lined paintings with full-field and in-situ capabilities.

Critical defects, including cuts, cracks, delaminations and detachments from lining supports in the paintings may degrade the structural integrity severely, and they may be barely or non-visible from the front and the reverse sides. Therefore, it is crucial to detect the presence of these defects early on [10–12] so that conservators can take action to monitor and prevent damage development and more accurately tailor to ensure the effectiveness of structural interventions.

A number of non-destructive techniques commonly used in conservation to identify sub-surface features and damage make use of X-rays. For example, X-ray radiography can visualise different painting constituents, internal structures and structural damage (e.g., cuts, cracks and insertions) [13,14]. By using radiography and tomography techniques, the preservation state of the paintings can be evaluated [13,14]. X-ray techniques, however, cannot reveal detachments, initiating and evolving defects [15]. Optical coherence tomography (OCT) is also commonly used in art conservation [13,16,17]. OCT can image and reconstruct the underlying layers in a painting, however, OCT has a limited penetration depth for deeper canvas layers and is a relatively slow process due to the limited field of view and the scanning procedure [11,16,17].

All the above-mentioned techniques provide potentially useful structural information to support conservation; however, there is a need to identify areas with strain and stress concentrations where internal defects and damage may affect the structural integrity of the painting.

Among the various optical inspection methods, holographic and speckle interferometry methods represented by holography, electronic speckle pattern interferometry (ESPI) and shearography offer the superior advantages of being non-contact, full-field and high sensitivity to the changes in shape or deformation. These techniques are mostly used for non-destructive inspection (NDI) in the aerospace industry [18–20]. In recent decades, they have also been adopted to detect defects and damage, such as cracks, fractures and detachments in paintings [21–25]. Of the three interferometry methods, shearography appears to be more practical for in-situ inspection [20,26]. It uses a common-path configuration which requires a simple optical setup and is insensitive to small rigid body motions and vibrations [20,26]. Furthermore, it directly measures derivatives of surface deformation under loading, which are closely related to surface strain components. This allows shearography to detect hidden defects and damage in underlying structures by monitoring the anomalies of the surface strain field, which is usually more reliable and practically more robust in-situ conditions than monitoring the anomalies of the surface displacement field as in classical holography or ESPI [20,26].

In most of the reported cases in cultural heritage, shearography was applied to measure only the out-of-plane or the in-plane strain components, e.g. for inspection of paintings on wooden panels, canvases and mural paintings [10,11,27–30]. Groves et al. developed a portable shearography sensor to study movable cultural heritage as museums regularly lend works of art to temporary exhibitions. Both panel and canvas paintings were measured with the aim of developing an impact assessment procedure [27]. Later Groves et al. combined shearography with terahertz imaging to evaluate a panel painting, providing both surface and bulk structural features for structural diagnostics [28]. Recently Gatto et al. adopted the shearography technique coupled with thermography to provide a holistic representation of the structural condition of a wall painting [29]. Most of the above-mentioned studies are qualitative inspections. There are limited reported results on the quantitative shearography NDI of paintings. Buchta et al. studied different loading methods and mechanisms including mechanical, thermal and humidity on the sensitivity of defects and damage detection in paintings [10]. Klausmeyer et al. used shearography to quantify and map strain on canvas paintings during changes in exhibition conditions [30]; however, only the surface paint layers were addressed. The novelty of this work is in the application of 3D shearography for the structural integrity inspection of wax-resin lined paintings for *The Night Watch*, enabling the full field monitoring of paintings in both in- and out-of-plane strain fields. Our preliminary results were reported earlier as conference proceedings [31].

In this paper, we present an inspection approach using 3D shearography for reliable identification and characterisation of defects and damage in wax-resin lined paintings for *The Night Watch*. The approach is to quantitatively analyse the in- and out-of-plane surface strain with controlled thermal excitation in the laboratory and in-situ environments. For the inspection, we used the previously reported 3D shape shearography instrument [32]. *The Night Watch* and a lined test painting with similarly repaired canvas cuts were inspected.

The need for excitation in shearography also raised questions about the safe loading procedure, specifically a safe raising of canvas temperature to achieve reliable inspection results without risks to the painting. In this research, we used thermal loading which offers the advantages of being non-contact, repeatable and controllable.

3. Materials and methods

3.1. The lined test painting

An anonymous twentieth-century canvas test painting (Fig. 1(a)), which was provided by the paintings conservation department at the Rijksmuseum, was used to evaluate the damage detection ability of the 3D shearography technique and to develop safe loading procedures for the NDI of paintings in the laboratory environment.

A transmitted light photo (Fig. 1(b)), taken by illuminating the back of the painting, highlights three parallel vertical slashes in the original canvas and one adjoining horizontal cut. The cuts in the canvas support of the test painting were joined together using thread 'bridges' dipped in a strong, rigid adhesive (epoxy resin) placed at small, regular intervals per cm. After drying and before

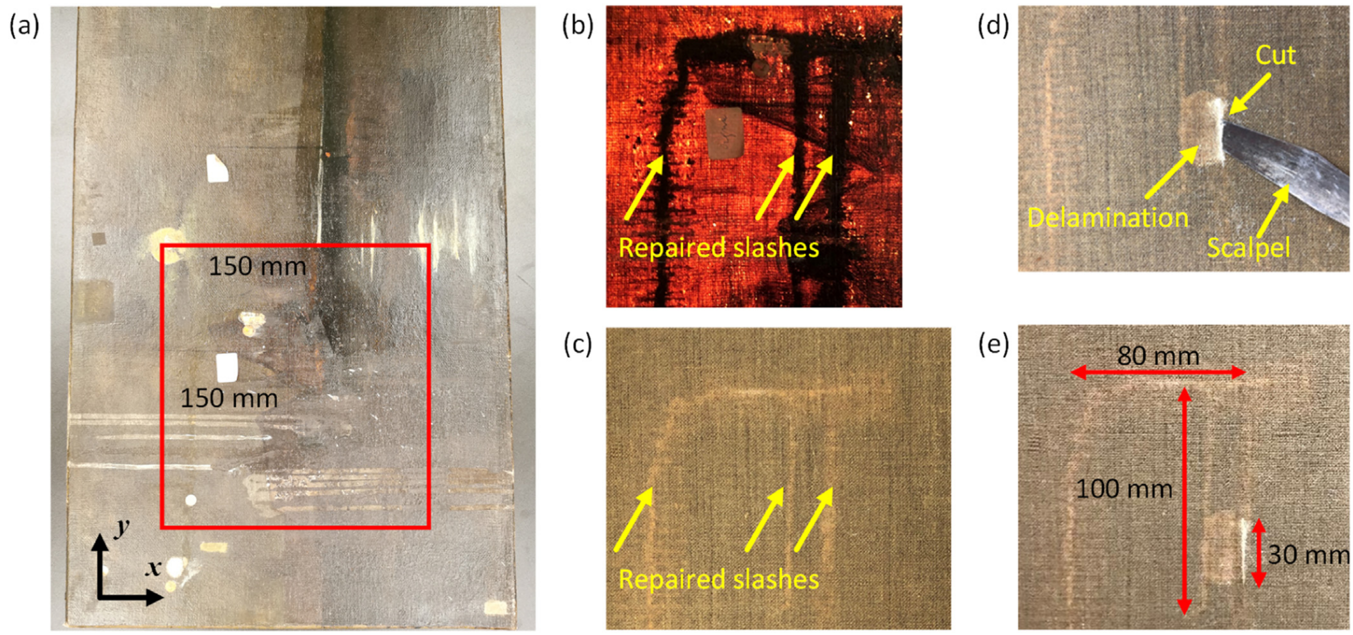

Fig. 1. The anonymous twentieth-century painting used for testing. (a) The test painting with the highlighted region of interest. (b) Transmitted light photo showing the repaired slashes using horizontal thread 'bridges'. (c) The reverse of the test painting before the intervention, (d) the intervention by a scalpel and (e) the cut and delamination. (b-d) horizontally flipped to match the photo in (a) directly.

relining, the threads would have been mechanically thinned with a scalpel. This painting was chosen as the tears in the canvas of the test painting have been repaired by using the same 'bridging' technique that was used to repair the slashes in *The Night Watch*. Like *The Night Watch*, the test painting was wax-resin relined with the second canvas. The repaired slashes are also partially visible through the lining canvas when observed from the reverse of the painting (Figs. 1(b,c)).

The purpose of the test painting was to create a relevant example for shearography inspection with reference defects to determine a safe thermal loading scenario with reliable defect detection. For that, an artificial delamination was made (Figs. 1(d,e)) by cutting the lining canvas with a scalpel and propagating an area of delamination between the canvases. This intervention resulted in two reference defects: first, the delamination between the original canvas and the lining canvas and, second, the in-plane canvas cut.

3.2. The Night Watch

For the following investigation, an in-situ structural integrity inspection with shearography was carried out in the galleries of the Rijksmuseum as a part of Operation Night Watch [9]. *The Night Watch* is a large oil on canvas painting with overall dimensions of 379.5 × 453.5 cm (Fig. 2). The original canvas support consists of three horizontal strips of canvas with two seams. Two inspected areas of interest, the Captain's breeches (approx. 0.5 × 1 m) and the drum (approx. 0.2 × 0.5 m), are marked in green and red, respectively. To minimise the exposure of the paint layers to the light and heat from the shearography thermal excitation source, these two areas were inspected from the reverse side.

3.3. Principles of 3D shearography

Shearography theory is well described in the literature [19,33,34]. Generally, shearography is used for the NDI of aerospace composite materials. To enable shearography inspection, a certain loading, e.g., thermal, mechanical or vibration is needed to deform the test object. This 3D shape shearography instrument was previously developed for surface strain measurement and material characterisation of free-form objects [32].

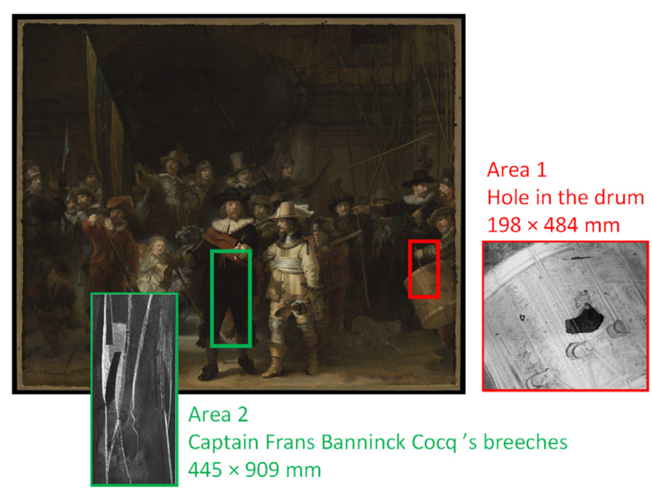

Fig. 2. Rembrandt van Rijn, *Officers and other civic guardsmen of District II in Amsterdam, under the command of Captain Frans Banninck Cocq and Lieutenant Willem van Ruytenburch*, known as '*The Night Watch*', 1642, oil on canvas, on long-term loan from the city of Amsterdam [8,9]. Areas 1 and 2 were inspected with 3D shearography.

During shearography inspection, a laser beam is expanded with a beam expander to illuminate an optically rough surface (Fig. 3(a)), creating a speckle pattern. When the shearing mirror is tilted by a small angle, two identical images separated by a shearing distance are generated. The scattered light from two adjacent points on the object surface interferes with each other in the image plane of a camera sensor, forming a speckle interferogram. In this paper, the shearing device with a Michelson interferometer is used as the shearing device due to its reliable adjustment of the shearing amount and shearing direction [19,34]. This shearing device also provides temporal phase-shifting of speckle interferograms for computing the corresponding optical phase change be-

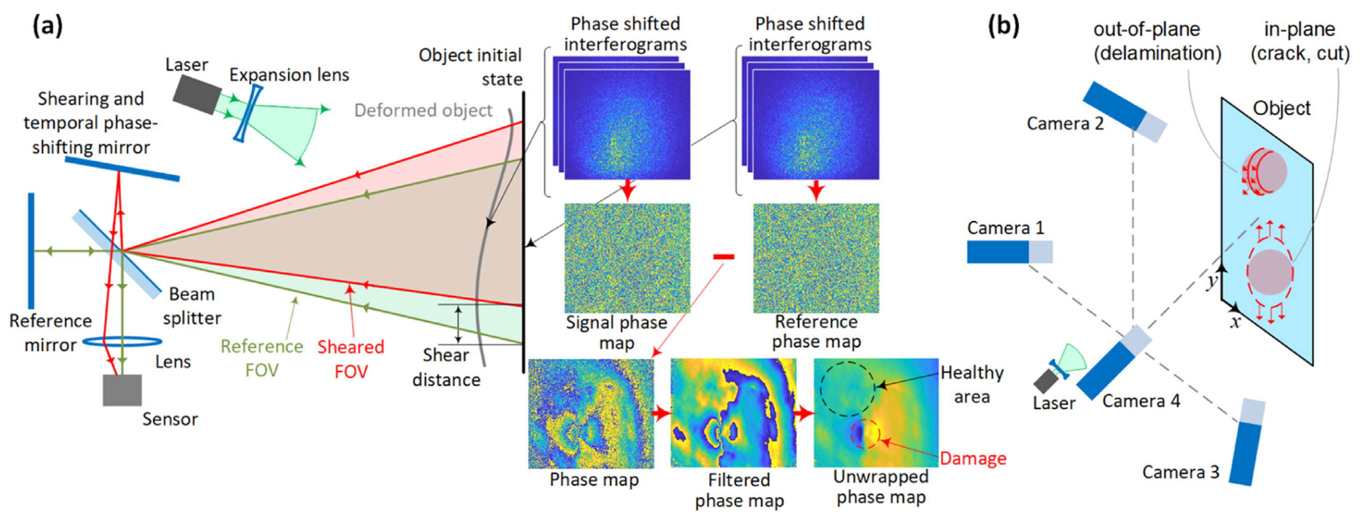

Fig. 3. Schematic of shearography principle. (a) Simplified optical scheme of the shearing camera with the Michelson interferometer and the data processing flow. (b) The spatial arrangement of shearing cameras in 3D shearography. FOV refers to field of view.

tween the initial and deformed object states. This phase map is then filtered and unwrapped to show a continuous surface displacement gradient map (Fig. 3(a)) [34]. Local variations in this map are often caused by defects and damage.

In 3D shearography, three shearing cameras (as in Fig. 3(a)) for three observation directions are used (cameras 1–3 in Fig. 3(b)), so that three surface strain components ($\partial u/\partial x, \partial v/\partial x, \partial w/\partial x$) can be independently derived for the shear in the x-direction [32]. When all cameras have the shearing direction along the y-axis, the surface strain components in the y-direction (e.g., $\partial u/\partial y, \partial v/\partial y, \partial w/\partial y$) are obtained. The ability to independently characterise the in- and out-of-plane surface strain components with 3D shearography enables the classification of damage and defects. From our experience, delaminations mostly cause out-of-plane deformations, while canvas cuts or cracks cause in- and out-of-plane variations (Fig. 3(b)). However, this classification capability of 3D shearography increases the complexity of the tests, the amount of data, and the processing time. Therefore, for certain tests only the out-of-plane behaviour was of interest and was determined with only one additional camera 4 (Fig. 3(b)), which is almost parallel to the laser direction and oriented perpendicular to the object's surface. This camera 4, when used alone, provides pure out-of-plane surface strain components ($\partial w/\partial x$ or $\partial w/\partial y$) depending on the shear direction.

3.4. 3D shearography instrument, phase processing and defect detection

The in-house built and modified 3D shearography instrument with four viewing and single illumination configuration is shown in Fig. 4(a). The instrument design and application cases were previously reported [29,32].

During the shearography inspection, the painting was illuminated with a Torus 532 laser (optical power set to 150 mW, wavelength of 532 nm by Laser Quantum) through expansion optics. The speckle pattern was imaged by four Pilot piA2400 cameras by Basler with Linos MeVis-C 1.6/25 lenses and Thorlabs bandpass filters. Each camera has a Michelson shearing interferometer with temporal phase-shifting realised by a piezo-electric actuator PSH 4z (Piezosystem Jena). The three-step phase shifting method was adopted due to its fast speed. Two halogen lamps (SUPER PAR CP62, maximum electrical power of 1 kW, correlated color temperature of 3200 K) were used for thermal excitation of the painting under inspection. The surface temperature was monitored with FLIR A655 IR camera. The individual field of view of each shearing camera was approximately 210 × 180 mm. Two shear distances were used: about 6 mm for the test painting in the laboratory environment for reliable damage detection and about 2.1 mm during the inspection of *The Night Watch*. The shear distance was reduced from 6 to 2.1 mm to enhance the stability of the shearography phase in the real environment. Given that the shear amount was significantly smaller than the distance to the painting (approximately 0.7 m), an assumption was made that the shearography phase maps correspond to the in- and out-of-plane surface strain components. This paper presents the shearography results in the units of phase (radians), which aligns with common practice in the field.

During the inspection, thermal excitation caused thermal expansion of the painting. The rise in temperature needed to be as low as possible but sufficient to cause strain anomalies to reliably detect defects. The following relaxation during cooling was continuously monitored to result in the shearography phase maps (Fig. 5). From our experience with thermal loading of canvas paintings, relatively long time delays between the temporal phase-shifted interferograms (e.g., longer than 20..30 s) cause phase discontinuities and loss of correlation due to rapid thermal deformation and vibrations. Faster acquisition (up to about 5 s) is sufficient to obtain resolvable phase maps, but multiple sets of interferograms have to be recorded over the cooling time (e.g. 100 sets in Fig. 5). Then the total phase map is calculated as a direct sum of the intermediate steps (total unwrapped phase map in Fig. 5). Further, the total phase map is compensated to remove the global deformation of the canvas [35,36] to highlight local phase anomalies (Fig. 5). During this compensation with the fitting of a smooth 2D polynomial surface into the phase map, a practical assumption is made that the global canvas deformations follow a smooth shape while local anomalies represent defects and damage [35,36].

In shearography inspection, there is no standard protocol or a fixed threshold for defect detection. First, in general, the higher the loading is, the higher the defect signal will be. Second, a local structural response may vary significantly in non-homogeneous materials (e.g., paintings) with varying thickness and structural composition. Third, the overall canvas deformation is significant, and the introduced phase compensation may not follow it precisely. Therefore, the phase interpretation is mainly done through expert analysis. In practice, the area in question may have a phase

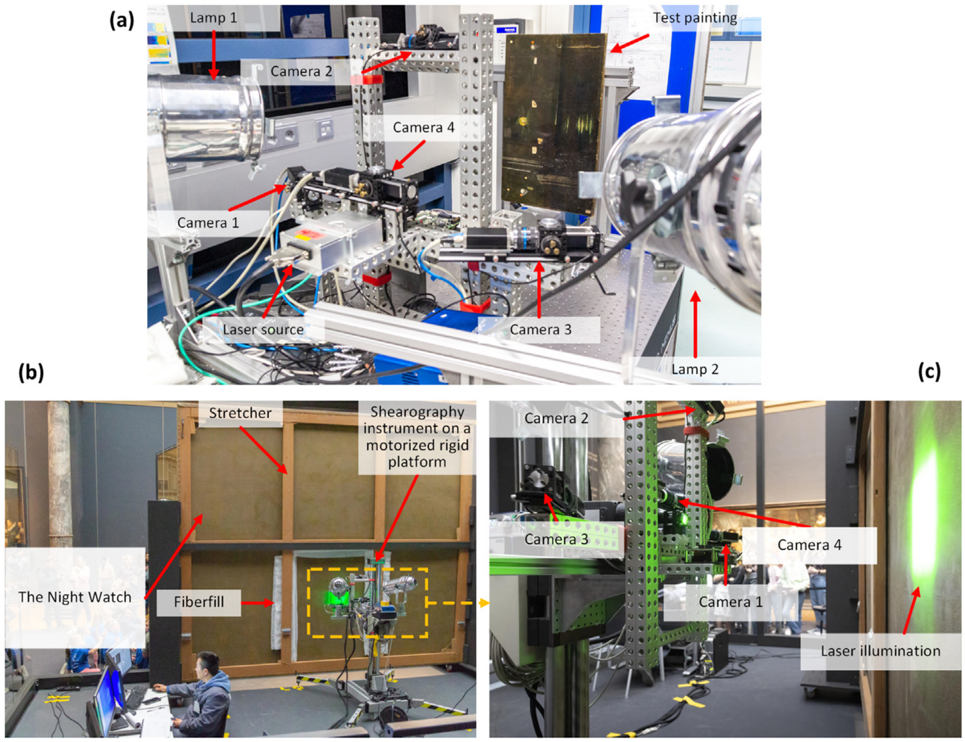

Fig. 4. 3D shearography instrument (a) in the lab with the test painting in front of it, (b,c) during the inspection of *The Night Watch* in the galleries of the Rijksmuseum with the shearography instrument mounted on a motorised stage.

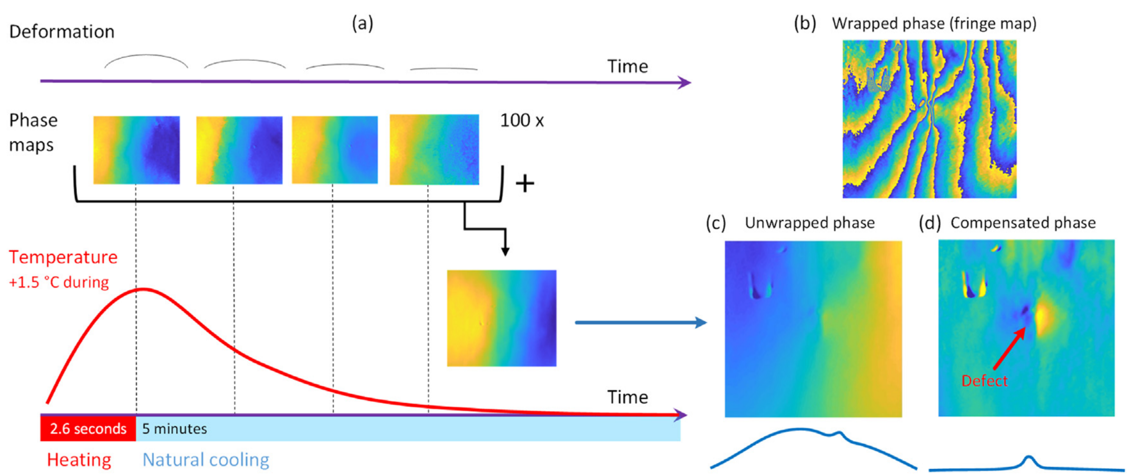

Fig. 5. Thermal loading and continuous measurements during cooling. The total sum of the unwrapped phase is compensated to reveal defects and damage.

signal with one or several shearography fringes (as in phase icons in Figs. 3 and 5; one phase fringe has a value of 2π or 6.28 radians).

For the in-situ inspection of *The Night Watch*, the 3D shearography instrument [32,37] was adapted and fixed on a motorised rigid platform (Figs. 4(b,c)) to enable controlled scanning of the painting and further image stitching. The inspection was done from the reverse side of the painting, and detailed reasoning was provided in Section 4.2.

The major practical issue during the inspection was the canvas vibrations. To alleviate the vibrations, two precautions were taken:

1) In the area of the Captain's breeches, a non-woven polyester padding material was placed in between the canvas and the stretcher bars surrounding the area (Fig. 4(b)) to provide local support to the canvas and, effectively, to dampen the vibrations. Vibrations in the drum area were at acceptable levels because this area is closer to the edge of the painting.
2) The ventilation system in the Night Watch Gallery of the Rijksmuseum and the airflow were found to be the main source of the canvas vibrations. During the measurements, the ventilation system was temporarily switched off.

4. Results and discussion

There are open research questions about developing safe loading procedures for the NDI of canvas paintings. For safety, the applied load, i.e., thermal excitation in this study, needed to be as minimal as possible. At the same time, the temperature increase has to be sufficient to cause strain anomalies to reliably detect damage. This section, first, reports the experimental inspection results for the test painting (Section 4.1). Threshold lim-

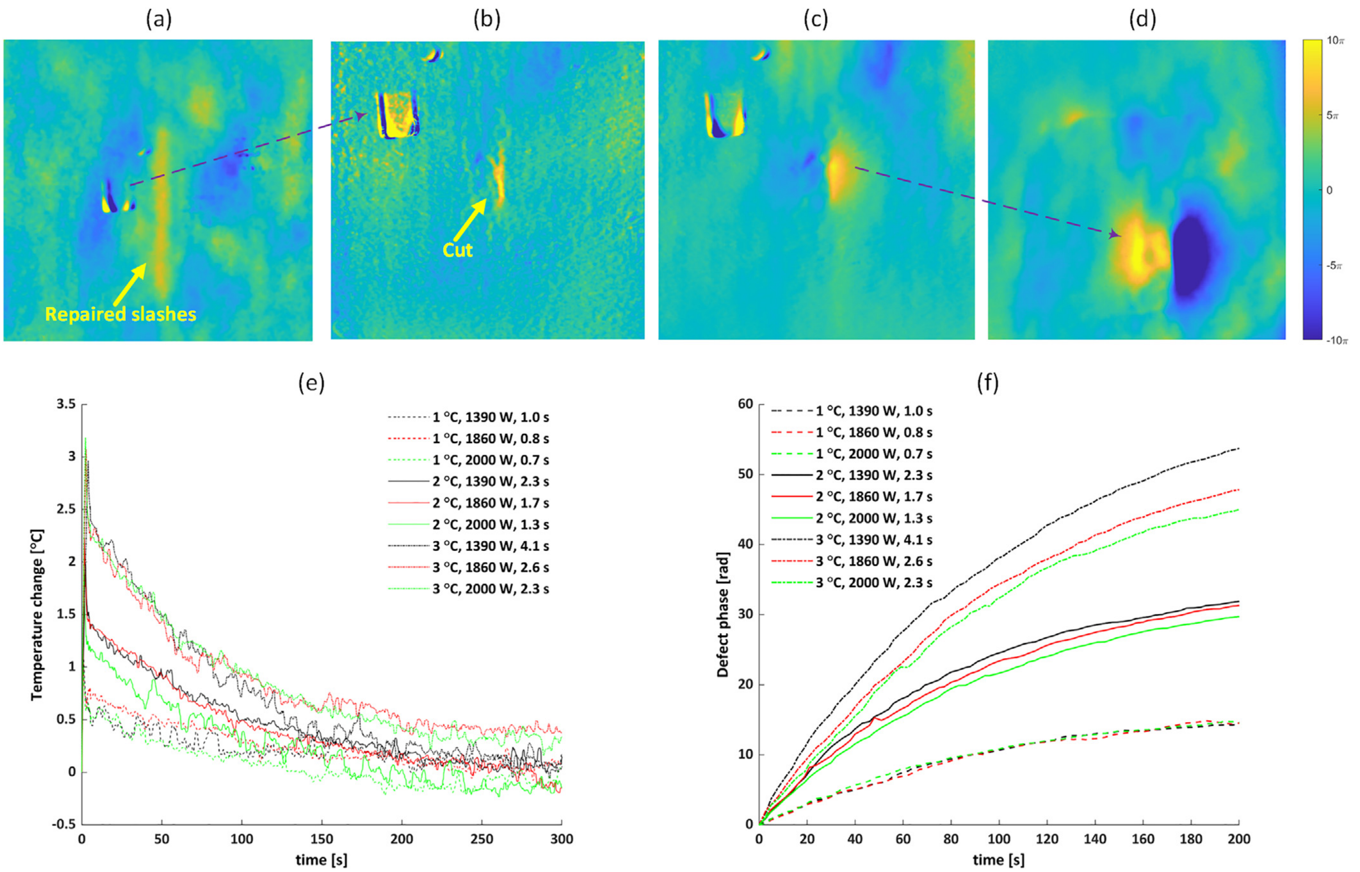

Fig. 6. Inspection phase maps, delamination-induced phase and the effective temperature increase. (a) Out-of-plane phase map before the cut (corresponding to $\partial w/\partial x$, inspected from the front, compensated). (b) In-plane phase map after the cut ($\partial u/\partial x$, front). (c) Out-of-plane phase map after the cut ($\partial w/\partial x$, front, compensated). (d) Out-of-plane phase map after the cut ($\partial w/\partial x$, reverse, compensated). (e) The surface temperature during thermal loading with varying power and the following cooling. (f) The dependence of the out-of-plane phase caused by the delamination from (c) on the heating power and heating time with controlled surface temperature increase.

its determined from the test painting have been further applied for the in-situ inspection of *The Night Watch* in the Rijksmuseum (Section 4.2).

4.1. Determining safe thermal loading scenario with reliable defect detection

To evaluate the efficiency of the 3D shearography inspection, the test painting was first inspected from the front and reverse before and after a cut and the area of delamination in the lining canvas were created (Fig. 1). During the inspection, the test painting was thermally loaded according to different scenarios (temperature increase of 1, 2, 3 °C) to determine a loading procedure for a safe inspection with reliable defect detection.

The test painting was preliminarily inspected from the front with only the out-of-plane configuration of the instrument (with only camera 4, Figs. 3,4). The repaired slashes in the canvas were detected in the compensated phase map (Fig. 6(a); the detected phase at the slash area was around 16–21 rad, with the overall canvas deformation around 240 rad). According to the shearography principle, vertical defects and features are more visible when the shear is applied in the horizontal direction, which is highlighted in Fig. 6(a) with the vertical repaired slashes.

Second, after the cut and delamination (Figs. 1(d,e)) were created in the lining canvas, the test painting was inspected with 3D shearography from the front (Figs. 6(b,c)). From the expectations and the results, the cut affects the in-plane strain field (corresponding to $\partial u/\partial x$), while the delamination affects the out-of-plane strain (corresponding to $\partial w/\partial x$). The intensity of the cut and delamination is around 36 and 30 rad, respectively, while the repaired slash (Fig. 6(a)) causes 16–21 rad. Therefore, the cut and the delamination cause higher strain concentrations and are easier to detect than the repaired slashes.

Third, the test painting with the cut and the delamination was inspected from the reverse side with the out-of-plane instrument configuration (Fig. 6(d)). The delamination causes comparable phase variations when inspected from the front and reverse sides (Figs. 6(c,d), respectively).

The presented phase levels of 16–21 rad for the repaired slashes and 30–36 rad for the cut and delamination correspond to several shearography fringes (2π or 6.28 rad each) and could be considered as detected defects in standard inspection practice. However, in this case, the overall canvas deformation is about 10 times higher (240 rad, about 40 fringes) than the signal from these areas of interest. When this significant overall deformation is compensated (Fig. 5), the compensated phase map reveals background phase variations of approx. ± 16 radians in known reference regions (Fig. 6(a); blue areas left and right from the vertical repair). These background variations can be explained by the local thickness and density differences which do not follow the smooth compensation curve.

Further, it was experimentally found that the phase caused by the delamination depends on the level of thermal excitation, which increases the canvas temperature to the same surface temperature with varying time. The test painting was thermally loaded with three power levels of 1390, 1860 and 2000 W (the total rated electric power of two halogen lamps and not the optical power) for different surface temperature increases of 1, 2 and 3 °C (Fig. 6(e)).

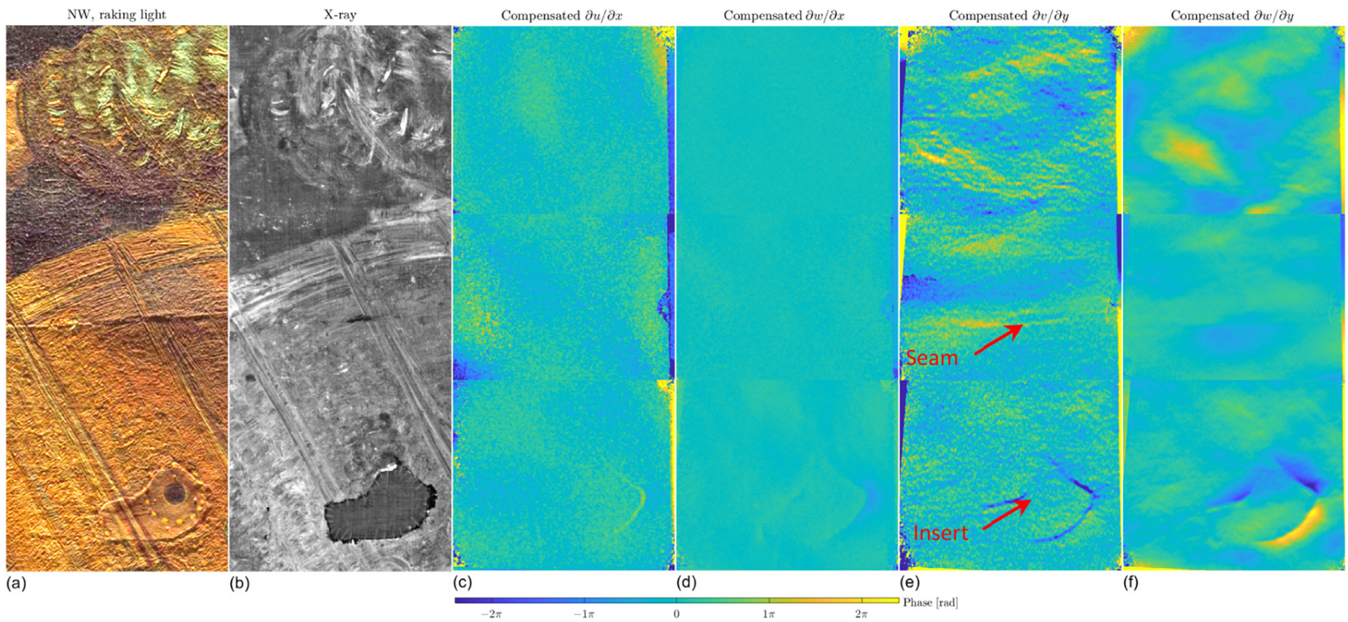

Fig. 7. 3D shearography inspection results of the drum area with the canvas seam and insert (198 × 484 mm). (a) Raking light image with corrected brightness and contrast, (b) X-ray radiography image of the same area with corrected brightness and contrast, (c) the in-plane $\partial u/\partial x$ and (d) the compensated out-of-plane phase maps $\partial w/\partial x$ with the shear in the x-direction (horizontal), (e) the in-plane $\partial v/\partial y$ and (f) the compensated out-of-plane phase maps $\partial w/\partial y$ with the shear in the y-direction (vertical).

The correspondent shearography phases caused by the delamination from Fig. 1(d) during these loading scenarios are presented in Fig. 6(f). For the temperature increase of 3 °C, the out-of-plane phase induced by the delamination increases if the thermal power decreases. So, slower thermal loading with less power up to the same temperature causes a higher defect signal. However, this effect decreases with the decrease of temperature change and is not resolved with a temperature increase of 1 °C.

Here are additional comments about the thermal loading. During these short exposures, the halogen lamps require a certain time to turn fully on and off. The presented thermal power levels are the desired set levels (e.g. 1390 W), so the maximum value. The duration, e.g. 2.3 s, includes the turn-on time and does not include comparable turn-off time. Also, the actual irradiance value from the halogen lamps on the painting surface was difficult to characterise. The corresponding illumination was measured with a light meter sensitive only to the visible part of the optical spectrum once the lamps were fully on. The power levels of 1390, 1860 and 2000 W correspond to approximately 24,000, 36,000 and 40,000 Lux in the central area of the test painting.

The intermediate results and discussion from the inspection of the test painting are:

1. A temperature increase of 1 to 2 °C is sufficient for reliable delamination detection in the test painting from the front and the reverse sides.
2. Phase compensation is needed to detect defects as the overall canvas deformation is significant. By doing this (as seen in the Figs. 5(c-d)), the overall deformation can be corrected from the data and the presence of defects can be identified and classified. Other techniques may be used to correct the overall deformation from the data: i) correcting the overall deformation by combining analytical solutions of thermal deformation or prediction by FEM, ii) combining a digital twin of the structure to correct the overall deformation, iii) Fourier transform analysis and/or principal component analysis may also be helpful.
3. Critical defects such as delaminations and cuts can be equally reliably detected from the front and the reverse sides. The old repairs in the canvas are also detectable. However, the background phase variation in reference regions is relatively high and may be misinterpreted as potential defects.
4. The paint layer buildup of the painting and its variation over the area (image contrast) and the varnish layer have limited effects on the inspection results.
5. Slow thermal exposure with reduced power resulting in the same temperature increase is beneficial as it induces a higher defect signal than faster (flash-like) exposure with high power. This is valid for 3D shearography as well as for conventional shearography techniques. In the future, the efficiency of slow thermal exposure can also be explored for active thermography [38–40].
6. The results also support the choice of the 3D shearography configuration for the simultaneous inspection of the in- and out-of-plane surface strain fields to potentially classify different defects (e.g. cuts vs delaminations).

4.2. *Inspection of* The Night Watch *at the Rijksmuseum*

Based on the results of the test painting (Fig. 6) and to further minimise risks, it was decided that the inspection of *The Night Watch* in the Rijksmuseum was done from the reverse side. The temperature of the selected area was gently raised up to 1.5 °C with 1390 W for 2.1 s to reliably detect potential delaminations. It was found that the expected thermal load time of 2.1 s had to be increased to 2.6 s to reach 1.5 °C. This was explained, first, by the lighter colour on the reverse side of *The Night Watch* compared to the front of the dark test painting with less absorption of the light and, second, that *The Night Watch* is effectively thicker than the test painting, so it has higher heat capacity.

Two areas of interest in *The Night Watch*, namely the canvas insert in the drum that is located close to one of the seams in the original canvas and the Captain's breeches with the repaired cuts were inspected with the 3D shearography system (Figs. 2 and 4). The final inspection results include in- and out-of-plane phase maps with the shear in the x-horizontal and y-vertical directions corresponding to the surface relaxation strain during cooling. These phase maps were calculated using the calibration informa-

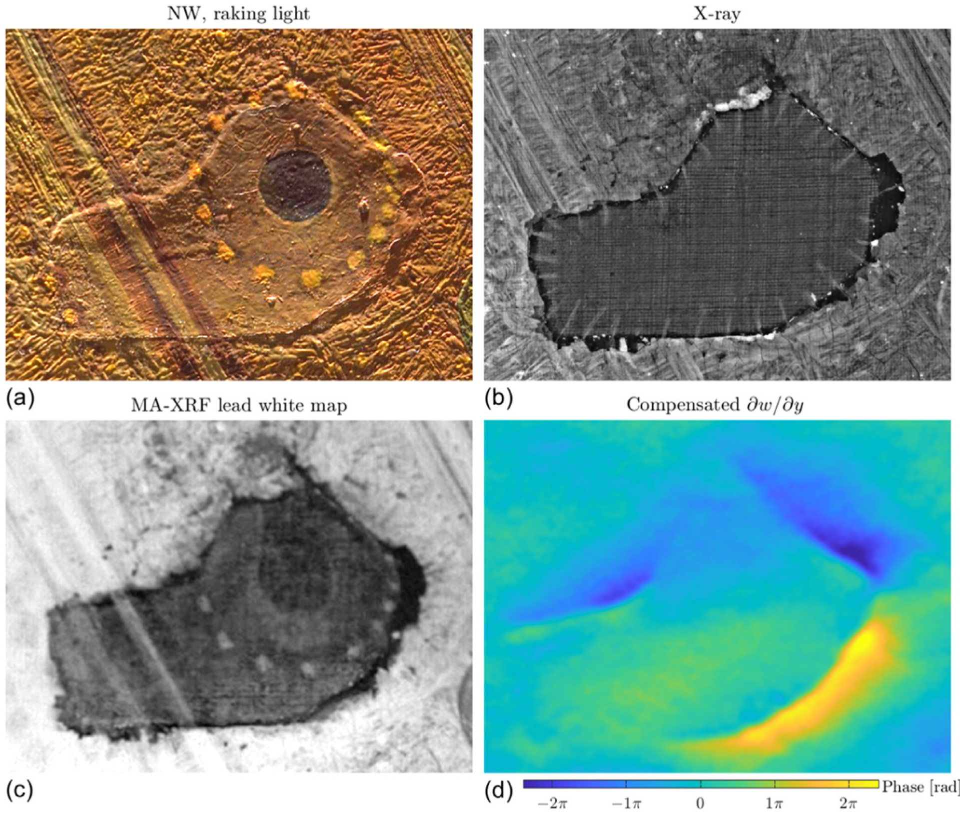

Fig. 8. Zoom into the inspection results of the drum insert. (a) Raking light image, (b) X-ray radiography image of the same area, (c) lead (Pb-L) map, macro X-ray fluorescence scanning spectroscopy (MA-XRF) associated with white lead. Brightness and contrast were corrected in (a-c). (d) The compensated out-of-plane phase map $\partial w/\partial y$ with the shear in the y-direction (vertical).

tion about the instrument geometry and 3D shearography processing methods [32,37].

The inspected area of the drum with the canvas insert and the seam in the original canvas support is shown in Fig 7(a). The inspected area is about 198 × 484 mm and consists of three fields of view that were inspected one after another and further stitched together to result in continuous phase maps. As the phase compensation is done independently for each field of view, the stitched map has minor offsets in phase values (seen as two horizontal lines). The seam and the canvas insert are detectable mostly in the in-plane $\partial v/\partial y$ and the out-of-plane $\partial w/\partial y$ phase maps (with the shear in the y-direction, Figs. 7(e,f)). The strain is the highest in the out-of-plane component with vertical shear and reaches 8.5 rad in the bottom right part (Fig. 7(f)). The zoomed-in inspection results of the drum insert are shown in Fig. 8.

The area investigated in the breeches of Captain Banninck Cocq (445 × 909 mm) was significantly larger than the drum area (198 × 484 mm), therefore inspection of the full area with 3D shearography was found not to be efficient from the time and effort points of view. The entire breeches area was inspected with the out-of-plane configuration of the instrument (Figs. 9(d, f)) to identify possible delaminations between the original canvas and the lining canvas, given the most severe slashes incurred in 1975 were concentrated in this area. In total 2 × 5 fields of view were stitched together. A smaller area, which was considered the most critical, was inspected with 3D shearography to result in-plane strain fields (Figs. 9(c, e)).

The inspection results of both investigated areas (Figs. 7 and 9) show that known structural features can be identified and mapped (viz. the seam in the original canvas and the insert in the drum, Fig. 7). The overall pattern of the repaired slashes in the breeches area can be traced in the out-of-plane phase map with the shear in the x-direction (red contour in Fig. 9(b) and white in $\partial w/\partial x$, Fig. 9(d)). The white dotted line in Fig. 9(d) is copied from the red contour in Fig. 9(b) for demonstration purposes. However, both the in-plane (Figs. 9(c, e)) and out-of-plane phase maps (Figs. 9(d, f)) do not have clear and significant local and sharp variations as compared to the area around the drum insert (Figs. 7(e, f)). If there were delaminations, higher localised phase signals would be expected (2–3 times higher than the signal from the repairs) following the effect of a delamination in the test painting (Fig. 6). The background variations (e.g. Fig. 9(f)) are the residuals from the phase compensation and can be explained by the local thickness and density differences.

In general, it is possible to use only shearography results for defect detection and classification as in Figs. 6(b-d). However defect detection in Figs 9(c-f) is challenging. From the shearography inspection results, no critical structural problems associated with the repaired slashes, nor with adhesion of the lining canvas, could be detected.

The discussion from the inspection of *The Night Watch*:

1. The results of the 3D shearography inspection from the reverse of the painting showed that the out-of-plane strain in the Captain's breeches does not show significant deviation that would indicate weakness in the adhesion between the repaired slashes and the lining canvas. The other repair, the canvas patch in the drum showed higher localised in- and out-of-plane strain variations. This can be explained by the less exacting repair of the hole in the canvas as compared to the repaired slashes in the breeches of Banninck Cocq.
2. Inspecting a large painting is more challenging than the small test painting. Vibrations and airflow are the main influencing parameters that affect in-situ shearography measurements. Ad-

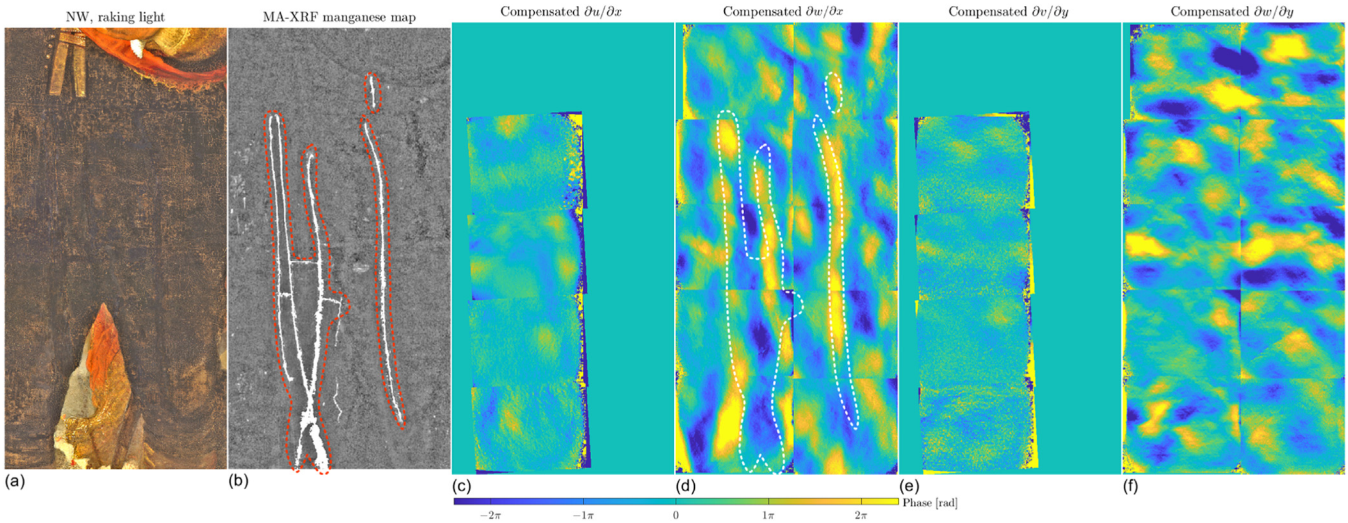

Fig. 9. 3D shearography inspection results of the Captain Banninck Cocq's breeches area (445 × 909 mm). (a) Raking light image with corrected brightness and contrast, (b) manganese (Mn-K) map, macro X-ray fluorescence scanning spectroscopy (MA-XRF) associated with the pigment umber used for repairing the slashes during the 1975–76 restoration with corrected brightness and contrast, (c) the in-plane $\partial u/\partial x$ and (d) the compensated out-of-plane phase $\partial w/\partial x$ with the shear in the x-direction (horizontal), (e) the in-plane $\partial v/\partial y$ and (f) the compensated out-of-plane phase $\partial w/\partial y$ with the shear in the y-direction (vertical).

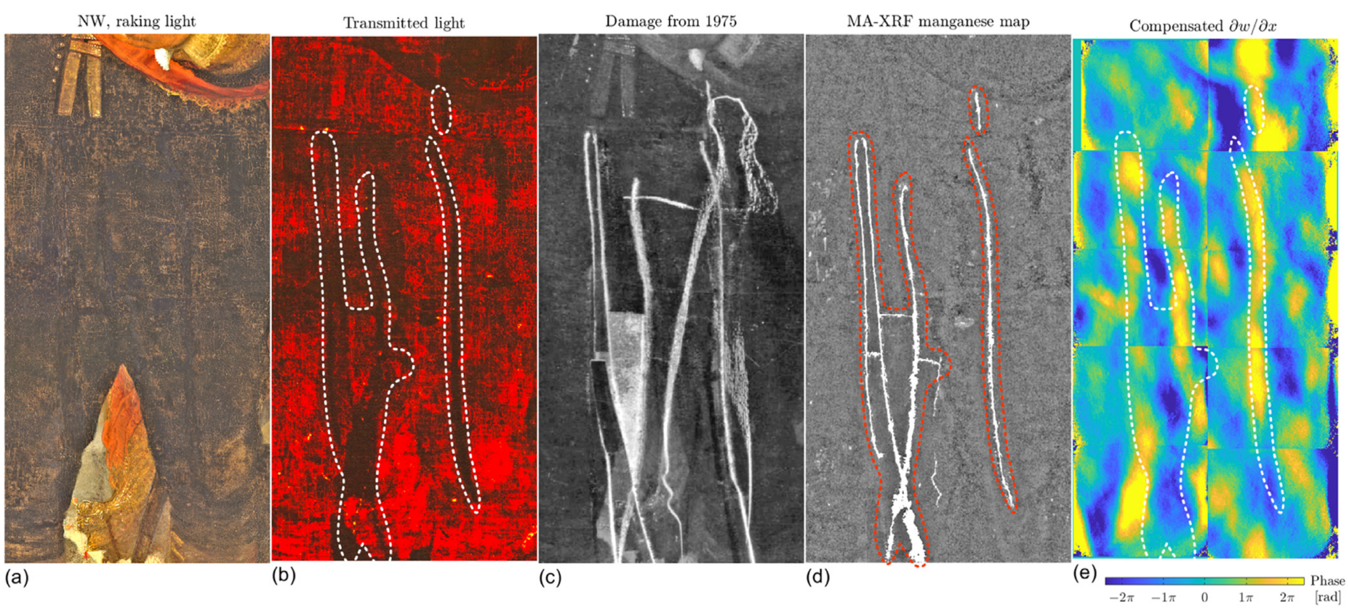

Fig. 10. Inspection results of the repaired slashes in Captain Banninck Cocq's breeches area (445 × 909 mm). (a) Raking light and (b) transmitted light images, (c) photo of the damage from 1975 before the tear repair, (d) manganese (Mn-K) map, macro X-ray fluorescence scanning spectroscopy (MA-XRF) associated with the pigment umber used for repairing the slashes during the 1975–76 restoration. Brightness and contrast were corrected in (a-d). (e) The out-of-plane phase map $\partial w/\partial x$ with the shear in the *x*-direction (horizontal, compensated).

ditional measures are needed to damp the vibrations up to a reasonable level, e.g., pauses in ventilation and additional canvas support. We expect that it is easier to inspect smaller paintings as lower vibration amplitudes are foreseen.

5. Conclusions

For the first time, 3D shearography has been used for the structural integrity inspections of wax-resin lined paintings, thus providing valuable information on structural integrity of the canvas support for their conservation and long-term preservation. For shearography, thermal loading by 1–2 °C is sufficient for reliable defect detection including delaminations, old cuts and other repairs. This rise in temperature is safe and acceptable, and comparable with normal fluctuations in temperature in the galleries, thus ensuring the safety of the paintings being tested. It was also shown that phase compensation is a needed process in defect detection that improves defect visibility and ease of detection. The compensation is needed due to significant canvas deformations (e.g., around 240 rad). This deformation is higher than a signal from the delamination (around 30 rad, Fig. 6) and significantly higher than the signal from the repaired stitches (around 16 rad, Fig. 6).

The intermediate conclusions were made based on the inspection of the test painting (Section 4.1). The main conclusions are as follows.

- From the inspection of the test painting, it was found that cuts and delaminations in canvas supports can be reliably detected

as in- and out-of-plane surface strain anomalies by raising the canvas temperature with 1 °C. Moreover, shearography was able to detect these defects from the front and the reverse sides. Cuts in the canvas mostly affect the in-plane strain distribution and delaminations – the out-of-plane strain. Therefore, 3D shearography can be used for defect classification.
- For the in-situ inspection of *The Night Watch* at the Rijksmuseum, 3D shearography with thermal loading was used to inspect two areas with restored damages, specifically the Captain Banninck Cocq's breeches and the drum. The non-destructive and non-contact inspection with 3D shearography provided valuable inspection results for assurances regarding the structural integrity of the 1975 repairs and the wax-resin relining, reducing the risks and providing the confidence to proceed with the planned retensioning of the canvas. The results shown here can act as a reference for new shearography inspections of *The Night Watch* or for other techniques.

Future work includes possible re-assessment of the structural integrity of *The Night Watch*, e.g., after a treatment as well as over time. It is also interesting to explore the effect of the natural climate variation in the galleries and to use it as a natural excitation for shearography inspection without additional thermal load.

Supplementary material

The most informative shearography results, namely the out-of-plane component $\partial w/\partial x$ (Fig. 9(d)), are presented as supplementary material in Fig. 10 together with the transmitted light image and photo of the damage from 1975 (Figs. 10(b,c)). The contours presented in Figs. 10(b,d,e) are the same as in Figs. 9(b,d).

Acknowledgements

We are indebted to Operation Night Watch team for making the X-ray radiography, raking light, the macro-X-ray fluorescence imaging spectroscopy and transmitted light data available. We acknowledge the main partner of Operation Night Watch – AkzoNobel. Operation Night Watch is made possible by The Bennink Foundation, C.L. de Carvalho-Heineken, PACCAR Foundation, Piet van der Slikke & Sandra Swelheim, American Express Foundation, Familie De Rooij, Het AutoBinck Fonds, TBRM Engineering Solutions, Dina & Kjell Johnsen, Familie D. Ermia, Familie M. van Poecke, Bruker Nano Analytics, Henry M. Holterman Fonds, Irma Theodora Fonds, Luca Fonds, Piek-den Hartog Fonds, Stichting Zabawas, Cevat Fonds, Johanna Kast-Michel Fonds, Marjorie & Jeffrey A. Rosen, Stichting Thurkowfonds, Familie Van Ogtrop Fonds, FedEx Express, Airbnb, NICAS, the Night Watch Fund, the City of Amsterdam and the Amsterdam Museum. The simulated damage and documentation of the test painting was carried out by Rijksmuseum paintings conservator, Giulia Sara de Vivo. We would also like to thank Wouter Lettinga for his preliminary results and active participation in the inspection process.

References

[1] E. Van Duijn, J.P. Filedt Kok, The restorations of Rembrandt's 'Night watch, in: J. Martineau, D. Bomford (Eds.), The Art of Conservation, The Burlington Press, London, 2024, pp. 268–303.
[2] M.Te Marvelde, 25.4 Waxresin lining, in: J.Hill Stoner, R. Rushfield (Eds.), The Conservation of Easel Paintings, Routledge Taylor & Franci, London/New York, 2021, pp. 450–459.
[3] M. Te Marvelde, How Dutch is 'The Dutch method'? A History of Wax-Resin Lining in its International Context, in: A. Oddy, S. Smith (Eds.), Past Practice – Future Prospects, The British Museum Occasional Paper 145, The British Museum Press, London, 2001, pp. 143–149.
[4] F. Gabrieli, J.K. Delaney, R.G. Erdmann, V. Gonzalez, A. van Loon, P. Smulders, et al., Reflectance imaging spectroscopy (RIS) for Operation Night Watch: challenges and achievements of imaging Rembrandt's masterpiece in the glass chamber at the Rijksmuseum, Sensors 21 (2021).
[5] M.F. Mecklenburg, Art in Transit: Studies in the Transport of Paintings, 1st edition, National Gallery of Art, 1991 https://scholar.google.com/scholar_lookup?title=Art%20in%20Transit%3A%20Studies%20in%20the%20Transport%20of%20Paintings&author=M.F.%20Mecklenburg&publication_year=1990.
[6] E. van Duijn, 'Like a Drunkard, the Diseased Painting Craved the Regenerating Alcohol ...' The Numerous Varnish Treatments of Rembrandt's 'The Night Watch' Between 1889 and 1936, in: idem, P. Noble (Eds.), Rembrandt Conservation Histories, 8th–9th November 2018, postprints, London and Amsterdam, 2021, pp. 138–151.
[7] P.J.J. van Thiel, Beschadiging en herstel van Rembrandts Nachtwacht /the Damaging and restoration of Rembrandt's Night Watch, Bull. van Het Rijksmus. 24 (1976) 4–13 http://www.jstor.org/stable/40381756. Accessed April 16, 2023.
[8] L. Kuiper, W. Hesterman, Restauratieverslag van Rembrandts Nachtwacht /Report on the restoration of Rembrandt's Night Watch, Bull. van Het Rijksmus 24 (1976) 14–51 http://www.jstor.org/stable/40381757. Accessed April 16, 2023.
[9] Rijksmuseum, Operation Night Watch, https://www.rijksmuseum.nl/en, (2019). https://www.rijksmuseum.nl/en/whats-on/exhibitions/operation-night-watch.
[10] D. Buchta, N. Hein, G. Pedrini, C. Krekel, W. Osten, Artwork inspection by shearography with adapted loading, Exp. Mech. 55 (2015) 1691–1704.
[11] D. Buchta, C. Heinemann, G. Pedrini, C. Krekel, W. Osten, Combination of FEM simulations and shearography for defect detection on artwork, Strain 54 (2018) e12269.
[12] D. Buchta, C. Heinemann, G. Pedrini, C. Krekel, W. Osten, "Lock-in-shearography for the detection of transport-induced damages on artwork," Proc. SPIE 10331, Optics for Arts, Architecture, and Archaeology VI, 103310G (11 July 2017); https://doi.org/10.1117/12.2270278.
[13] B. Borg, M. Dunn, A. Ang, C. Villis, The application of state-of-the-art technologies to support artwork conservation: literature review, J. Cult. Herit. 44 (2020) 239–259.
[14] C. Calza, D.F. Oliveira, R.P. Freitas, H.S. Rocha, J.R. Nascimento, R.T. Lopes, Analysis of sculptures using XRF and X-ray radiography, Radiat. Phys. Chem. 116 (2015) 326–331.
[15] R.M. Groves, B. Pradarutti, E. Kouloumpi, W. Osten, G. Notni, 2D and 3D non-destructive evaluation of a wooden panel painting using shearography and terahertz imaging, NDT E Int 42 (2009) 543–549.
[16] T. Callewaert, J. Guo, G. Harteveld, A. Vandivere, E. Eisemann, J. Dik, et al., Multi-scale optical coherence tomography imaging and visualization of Vermeer's Girl with a pearl earring, Opt. Express 28 (2020) 26239–26256.
[17] M. Maria, A.G. Anisimov, M. Stols-Witlox, R.M. Groves, "Analysis of a SD-OCT-based hyperspectral system for spectral reflectance measurements," Proc. SPIE 11354, Optical Sensing and Detection VI, 113541J (1 April 2020); https://doi.org/10.1117/12.2555435.
[18] W. Osten, G. Pedrini, 55 Years of holographic non-destructive testing and experimental stress analysis: is there still progress to be expected? Light Adv. Manuf. 3 (2022) 121–136.
[19] D. Francis, R.P. Tatam, R.M. Groves, Shearography technology and applications: a review, Meas. Sci. Technol 21 (2010) 102001.
[20] W. Steinchen, L. Yang, G. Kupfer, P. Mäckel, Non-destructive testing of aerospace composite materials using digital shearography, Proc. Inst. Mech. Eng. Part G J. Aerosp. Eng. 212 (1998) 21–30.
[21] D. Ambrosini, D. Paoletti, Holographic and speckle methods for the analysis of panel paintings. Developments since the early 1970s, Stud, Conserv 49 (2004) 38–48.
[22] C. Ibarra-Castanedo, S. Sfarra, D. Ambrosini, D. Paoletti, A. Bendada, X. Maldague, Diagnostics of panel paintings using holographic interferometry and pulsed thermography, Quant. Infrared Thermogr. J. 7 (2010) 85–114.
[23] S. Amadesi, F. Gori, R. Grella, G. Guattari, Holographic methods for painting diagnostics, Appl. Opt. 13 (1974) 2009–2013.
[24] Ł. Lasyk, M. Łukomski, T.M. Olstad, A. Haugen, Digital speckle pattern interferometry for the condition surveys of painted wood: monitoring the altarpiece in the church in Hedalen, Norway, J. Cult. Herit. 13 (2012) S102–S108.
[25] L. Krzemień, M. Łukomski, A. Kijowska, B. Mierzejewska, Combining digital speckle pattern interferometry with shearography in a new instrument to characterize surface delamination in museum artefacts, J. Cult. Herit. 16 (2015) 544–550.
[26] Y.Y. Hung, L.X. Yang, Y.H. Huang, Non-destructive evaluation (NDE) of composites: digital shearography, in: V.M. Karbhari (Ed.), Non-Destructive Eval, Polym. Matrix Compos., Woodhead Publishing, 2013, pp. 84–115.
[27] R.M. Groves, W. Osten, M. Doulgeridis, E. Kouloumpi, T. Green, S. Hackney, V. Tornari, "Shearography as part of a multi-functional sensor for the detection of signature features in movable cultural heritage," Proc. SPIE 6618, O3A: Optics for Arts, Architecture, and Archaeology, 661810 (19 July 2007); https://doi.org/10.1117/12.727497.
[28] R.M. Groves, B. Pradarutti, E. Kouloumpi, W. Osten, G. Notni, "Multi-sensor evaluation of a wooden panel painting using terahertz imaging and shearography," Proc. SPIE 7391, O3A: Optics for Arts, Architecture, and Archaeology II, 73910E (10 July 2009); https://doi.org/10.1117/12.827528.
[29] V. Gatto, A.G. Anisimov, W. Lettinga, N. Tao, M. Lantman, B. Crijns, R.M. Groves, "Application of shearography and the percussion method for the structural inspection of wall paintings: a case study of St. Christopher in Maria Church, Nisse," Proc. SPIE 11784, Optics for Arts, Architecture, and Archaeology VIII, 117840K (8 July 2021); https://doi.org/10.1117/12.2591911.
[30] P. Klausmeyer, M. Cushman, I. Dobrev, M. Khaleghi, E.J. Harrington, X. Chen, et al., Quantifying and mapping induced strain in canvas paintings using laser shearography, Noninvasive Anal. Paint. Surfaces Sci. Impact Conserv. Pract. (2016) 1–13.

[31] N. Tao, A.G. Anisimov, E. van Duijn, L. Vos, I. Steeman, K. Keune, P. Noble, R.M. Groves, Application of shearography with thermal loading for the structural inspection of Rembrandt's Night Watch, Proc. SPIE 12620, Optics for Arts, Architecture, and Archaeology (O3A) IX, 126200A (9 August 2023). https://doi.org/10.1117/12.2673263.
[32] A.G. Anisimov, M.G. Serikova, R.M. Groves, 3D shape shearography technique for surface strain measurement of free-form objects, Appl. Opt. 58 (2019) 498–508.
[33] Y.Y. Hung, Shearography: a new optical method for strain measurement and nondestructive testing, Opt. Eng. 21 (1982) 391–395.
[34] W. Steinchen, Digital shearography: theory and application of digital speckle pattern shearing interferometry, SPIE Press, Bellingham, WA, USA, 2003.
[35] N. Tao, A.G. Anisimov, R.M. Groves, Shearography non-destructive testing of thick GFRP laminates: numerical and experimental study on defect detection with thermal loading, Compos. Struct. 282 (2022) 115008.
[36] N. Tao, A.G. Anisimov, R.M. Groves, FEM-assisted shearography with spatially modulated heating for non-destructive testing of thick composites with deep defects, Compos. Struct. 297 (2022) 115980.
[37] A.G. Anisimov, B. Müller, J. Sinke, R.M. Groves, Analysis of thermal strains and stresses in heated fibre metal laminates, Strain 54 (2018) e12260.
[38] S.B. Tombet, E. Guyot, R. Huillery, T. Calligaro, V. Detalle, X. Bai, et al., Active thermography for panel paintings inspection: a comparative study of mid-wave and long-wave infrared spectral analysis, in: Proc. 16th Quant. InfraRed Thermogr. Conf, 2022, pp. 4–8.
[39] H. Kouser, S.B. Tombet, J. Carrock, V. Detalle, T. Calligaro, X. Bai, C.Y. Cergy, in: Pulse Phase Thermography for Panel Paintings Inspection in Mid-wave and Long-wave Infrared Bands, Abu Dhabi, UAE, 2023.
[40] S. Kunikata, Y. Tsuchiya, K. Fukunaga, Comparison of non-destructive examination methods for wax-resin lining of paintings on canvas, in: 2022 47th Int. Conf. Infrared, Millim. Terahertz Waves, 2022, pp. 1–2.